Nano Energy 92 (2022) 106756

Contents lists available at ScienceDirect

Nano Energy

journal homepage: www.elsevier.com/locate/nanoen

# COFs-based electrolyte accelerates the $Na^+$ diffusion and restrains dendrite growth in quasi-solid-state organic batteries

Genfu Zhao [a], Lufu Xu [a], Jingwen Jiang [a], Zhiyuan Mei [a], Qi An [a], Pengpeng Lv [c,*], Xiaofei Yang [b], Hong Guo [a,*], Xueliang Sun [b,*]

[a] School of Materials and Energy, Yunnan University, Kunming 650091, China
[b] Nanomaterials and Energy Lab Department of Mechanical and Materials Engineering, Western University, London, Ontario N6A 5B9, Canada
[c] State Key Laboratory of Multiphase Complex Systems, Institute of Process Engineering, Chinese Academy of Sciences, Beijing 100190, China

ARTICLE INFO

*Keywords:*
Covalent organic frameworks
Na-ion conductor
Quasi-solid-state organic batteries

ABSTRACT

Solid-state sodium-ion batteries exhibit a great promising opportunity for the future energy storage, and thus exploring a high-efficiency sodium-ion conductor is the urgent challenge. Covalent organic frameworks (COFs) have accurately directional and well-defined ion channels and are a promising and optimal platform for solid-state Na-ion conductor. In this work, we study the first example of carboxylic acid sodium functionalized polyarylether linked COF (denoted as NaOOC-COF) as an advanced Na-ion quasi-solid-state conductor film. Benefiting from the well-defined ion channels, the functionalized NaOOC-COF exhibits an outstanding $Na^+$ conductivity of $2.68 \times 10^{-4}$ S $cm^{-1}$ at room temperature, low activation energy (Ea) with 0.24 eV and high transference number of 0.9. Particularly, the NaOOC-COF shows long-time cycling performance in the assembled quasi-solid-state battery, and can restrain dendrite growth through interface regulation. Furthermore, the $Na^+$ diffusion mechanism in whole-cell system is investigated thoroughly. Such extraordinary Na-ion transport result based on COFs is achieved for the first time. This novel strategy may exploit the new area of Na-ion quasi-solid-state electrolytic devices, and simultaneously accelerate the progress of functionalized COFs.

## 1. Introduction

Energy storage systems (EESs) increasingly play a crucial role in our daily life, which can provide us convenient and rapid functions [1–5]. Among them, sodium-ion batteries are a novel great promising energy storage system for the electric vehicles and smart grids, due to its low cost and sustainability. However, it encounters serious efficiency and safety troubles because sodium shows high activity and dendrite is easy formation in traditional liquid electrolyte system. Therefore, the development of solid-state or quasi-solid-state Na-ion batteries could avoid electrolyte leaking and restrain dendrite growth through interface regulation, and thus render the battery with more safety and high energy density and power [6–20].

Solid electrolytes (SEs) are the key bottleneck in solid-state NIBs. Though, inorganic solid electrolytes (ISEs) have high ionic conductivity, their poor electrode surface wettability would not only entail a large interface resistance, also cause the growth of Na dendrite along the grain boundary [21,22]. Contrast with ISEs, solid polymer electrolytes (SPEs), which are homogeneous mixtures of Na salts and solid polymers with relatively high molecular weight, are characterized by the excellent compatibility with electrode materials, flexibility, light weight and low-cost processing. However, the presence of freely mobile anions and organic solvents inevitably gives rise to unwanted interfacial side reactions, impedes the Na-ion migration and conductivity (Fig. 1a), thus leading to bad effects for the practical utilization. Moreover, SPEs are not steady in harshly chemical environment.

To tackle these bottlenecks, designing a highly stable Na-ion conductor is the key technology. Except for conventional ISEs and SPEs, which are at the relatively mature studying stage, a new burgeoning type of solid-state ion conductor, covalent organic frameworks (COFs) based polymeric crystalline porous material are attracting more and more attention over the past decade. They are a sort of porous and crystalline 2D material with precisely chemical modification and applied in various fields [23–29]. Its outstanding structure stability of COFs can maintain service life of cells [30–32]. What is more, the well-defined ion channels can provide a favorable environment for the

* Corresponding authors.
*E-mail addresses:* lvpengpeng@ipe.ac.cn (P. Lv), guohong@ynu.edu.cn (H. Guo), xsun9@uwo.ca (X. Sun).

https://doi.org/10.1016/j.nanoen.2021.106756
Received 5 September 2021; Received in revised form 31 October 2021; Accepted 15 November 2021
Available online 24 November 2021

metal ion migration, which is beneficial to enhance the ion conductivity [33–39]. Furthermore, the feature of easily chemical modification for COFs leads to the anionic segment easily covalently tethered in the cavity of COFs, improving $Na^+$ ionic transference number. Meanwhile, the directional and well-defined ion channels play a crucial foundation for Na-ion fast transport and migration. As a consequence, COFs are a promising, ideal and optimal platform for solid-state Na-ion conductors. However, the related research on COFs-based SSEs still in its early stages. Particularly, most of COFs-based SSEs are focused on lithium-ion batteries, while little reports on NIBs. Meanwhile, they exist the drawbacks of poor mechanical strength, high activation energy, and small ionic transference number. Moreover, the current reported COFs linked through C═N or C-N exhibit unstable structure performance in battery systems. Therefore, constructing unique COFs-based Na-ion conductor for solid-state NIBs, possessing high ion conductivity, enhanced mechanisms, flexible property, low activation energy and wide electrochemical widow, is a big challenge and highly desired.

Hence, we report carboxylic acid sodium functionalized COF as an advanced Na-ion conductor flexible film (Fig. 1b-g) used in quasi-solid-state organic sodium metal batteries for the first time as far as our knowledge. The C═N modified COF (NC-COF) is obtained by ether linkage between 2,3,6,7,10,11-hexahydroxytriphenylene hydrate (HHTP) and tetrafluoroterephthalonitrile (TFTPN) in the triethylamine as base at 120 °C for 3 d. Then, after hydrolysis of NC-COF in aqueous NaOH, the NaOOC-COF can be obtained. The carboxylic acid group is covalently tethered in the cavity of COF to enable $Na^+$ conduction [40,

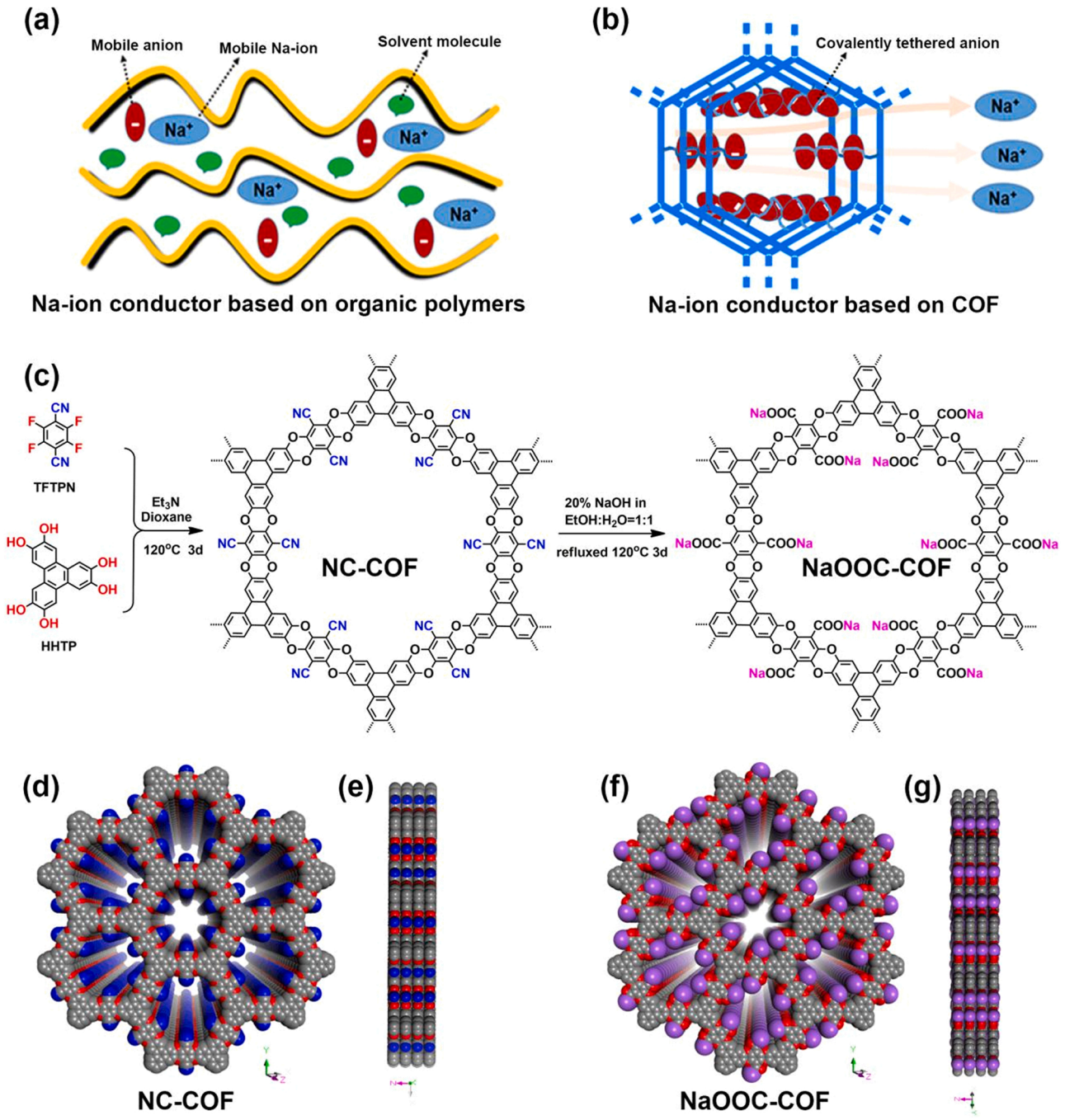


**Fig. 1.** Na-ion conductor supported by organic polymers with addition of sodium salts and solvents (a); single Na-ion conductor based on COF (b); synthetic route of NC-COF and NaOOC-COF (c); top views of NC-COF (d) and NaOOC-COF (f) and side views of NC-COF (e) and NaOOC-COF (g).

41]. Compared with previous reported COFs containing B-O, C═N and C-N bonds, this unique framework assembled by ether bonds (C-O-C) connection illustrates highly chemical stability in various harsh environment, and mechanical robustness [42]. In consequence, the prepared NaOOC-COF is reasonably made to weaken the side reaction between electrode and electrolyte, and thus impede the growth of sodium dendrite. Simultaneously, this COFs could make amends for the flammable drawback of polymer SSE. Meanwhile, NaOOC-COF establishes an anionic skeleton with directional ion channel, generating free single $Na^+$ migration. Therefore, it is benefit for the enhancement of sodium ionic transference number, and reduces the polarization resulted from different ion concentration gradient as well, thus increasing the stability of electrode/electrolyte interface. Furthermore, this COF exhibits unique two-dimensional extended layered structure and self-assembled well-defined one-dimensional ion channels. These features can enhance the content of Na-ion in SSE, improve the Na-ion dynamic

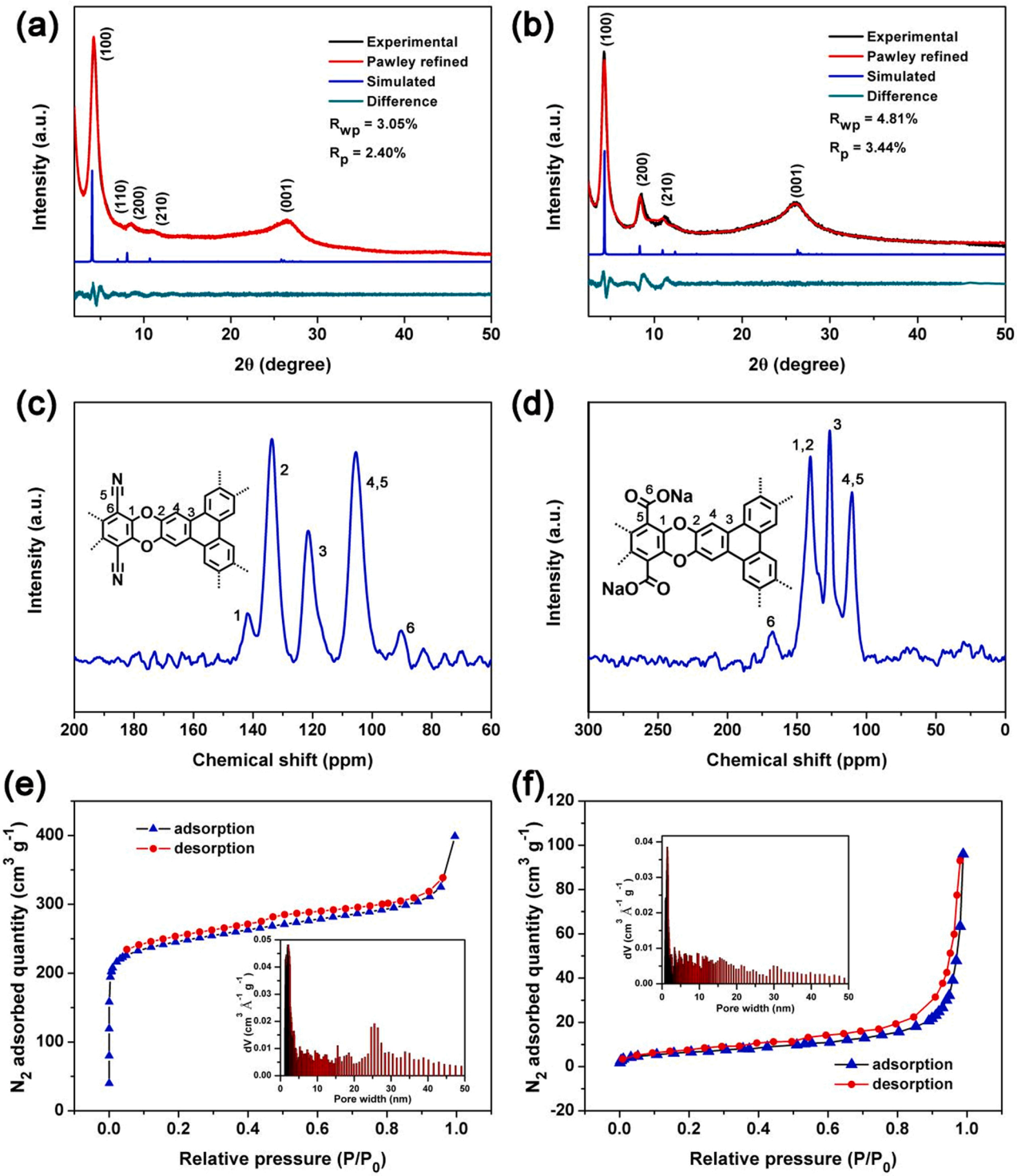


**Fig. 2.** PXRD patterns of NC-COF with experimental, simulated Pawley refined results (a); PXRD patterns of NaOOC-COF with experimental, simulated Pawley refined results (b); solid-state $^{13}C$ NMR spectrum of NC-COF (c) and NaOOC-COF (d); $N_2$ adsorption-desorption isotherm for NC-COF (e) and NaOOC-COF (f). Inset: pore size distribution from fitting the NLDFT model to the adsorption data.

behavior, promote the Na-ion migration and shorten the Na-ion hopping distance, thereby further improve the Na-ion conductivity and decrease the activation energy. So, the prepared COFs-based Na-ion conductor is assembled into quasi-solid-state organic Na-ion batteries to expect enhanced electrochemical performance. The degree of negative charge delocalization, diverse skeleton structure and charge difference have great influence on the electrochemical behaviors, and thus these factors are studied through DFT theoretical calculation deeply. Moreover, a clear understanding of the mechanism of Na-ion transportation is provided to thoroughly break through the key bottlenecks of COFs-based structured $Na^+$ conductor electrolytes in SSNIBs.

## 2. Results and discussions

Powder X-ray diffraction (PXRD) is carried out to study the crystallinity of synthesized NC-COF and NaOOC-COF. As exhibited in Fig. 2a, the PXRD pattern of NC-COF presents relevant peaks at $2\theta = 4.2$, 7.23, 8.51, 11.05 and 26.51°, attributed to the (100), (110), (200), (210) and (001) planes, respectively [40,41]. Moreover, the experimental result matches commendably the simulated pattern (AA stacking), but is not well satisfied another alternative arrangement (AB stacking), meaning the AA stacking drives the structure of NC-COF (Fig. S1−3). After hydrolysis of NC-COF, the PXRD pattern of production of NaOOC-COF can also show these same peaks at $2\theta = 4.23$, 8.5, 11.13 and 26.12°, which implies that NaOOC-COF has similar crystalline structure with NC-COF. We also launch the calculated PXRD pattern of NaOOC-COF, demonstrating the AA stacking drives the structure (Fig. S4−6). In addition, the simulated patterns of NC-COF and NaOOC-COF almost have the same profile (Fig. S7). Finally, we launch the full profile pattern matching (Pawley) refinements versus the experimental PXRD patterns of NC-COF (Fig. 2a, red and black curve) and NaOOC-COF (Fig. 2b, red and black curve), which yields good result of refinement and experiment. This result can be further proved the crystalline structure. On the basis of above consequences, the chemical modification of NC-COF does not alter the eclipsed stacking architecture. And this eclipsed stacking architecture is mainly generated by the vigorous trend of hexahydroxytriphenylene centers aggregates [40].

Fourier-transform infrared (FTIR) spectroscopy is used to analyze these characteristic peaks of −OH, −C≡N and −C═O groups. Fig. S8 displays the adsorption peaks at wavenumber of 1261 and 1019 $cm^{-1}$. The two peaks are generated from the asymmetric and symmetric vibration of ether bonds on the NC-COF. Additionally, the peak at 2241 $cm^{-1}$ of NC-COF is ascribed to the C≡N stretching, and the obvious weaken of OH peak at 3429 $cm^{-1}$ can be found in the initiatory substance of HHTP [40,41]. These results can present a powerful evidence that starting materials of HHTP and TFTPN have been highly transformed into the polymerizations of NC-COF. Noteworthily, the adsorption peak of C≡N disappears distinctly after the hydrolysis of NC-COF and another new peak appears at 1685 $cm^{-1}$ in the final product of NaOOC-COF, implying thorough conversions from the NC-COF to NaOOC-COF (Fig. S9) [40,41]. Based on the above analysis, we further evaluate the chemical conversions procedure by the solid-state $^{13}C$ cross-polarization magic-angle spinning (CP-MAS) NMR. As shown in Fig. 2c, the chemical shift at ~110 ppm is attributed to C specie in C≡N segment [40,41]. When the C≡N group is hydrolysed, a fresh peak can be observed at ~164 ppm (Fig. 2d), corresponding to the carboxylic acid [41]. This important result can further prove above conclusion.

The porousness of synthesized samples NC-COF and NaOOC-COF are measured by the nitrogen adsorption–desorption implemented at 77 K. An apparent type I isotherm can be seen for NC-COF material, indicating microporous feature (Fig. 2e) [40,41]. Similar nitrogen adsorption–desorption curve appears for NaOOC-COF sample (Fig. 2f), which illustrates that the chemical modification does not affect for the microporous trait. According to the non-local density functional theory, the pore size distribution of NC-COF shows pore with diameter of ~1.6 nm (Fig. 2e, inset). However, the pore size slightly decreases for NaOOC-COF from 1.6 to 1.56 nm (Fig. 2f, inset), which might assign to the distributions of Na-ions in the framework of NaOOC-COF. BET plot of NC-COF reveals a surface area of 785 $m^2\ g^{-1}$ calculated from $N_2$ adsorption isotherm at 77 K. The NaOOC-COF has relative lower surface area of 102 $m^2\ g^{-1}$ than NC-COF, this change can be attributed to enhancing the amount density of Na-ions and the crystallinity for NaOOC-COF is inevitably decreased than NC-COF, caused by the chemical modification. From the CN group to the COONa group, the volume of metal Na-ion and carboxyl is obviously larger than CN group. Therefore, the crystallinity, BET surface and pore size for NaOOC-COF slightly decreases. X-ray photoelectron spectroscopy (XPS) is used to certify this chemical modification procedure. As demonstrated in Fig. S10, the XPS survey for NC-COF displays C, N, O elements and little F. The limited F reveals complete conversation of starting materials of TFTPN and HHTP. XPS of C 1 s for NC-COF illustrates C≡N, C═C and C–O bonds, implying high accordance with the chemical composition (Fig. S11). More importantly, after hydrolysis of NC-COF, XPS survey of NaOOC-COF shows C, O and Na elements, and the almost no N element can be detected, which is caused by the fact that –CN groups in NC-COF are completely conversed into –COONa groups (Fig. S10). In addition, XPS of C 1 s for NaOOC-COF reveals C═C, C–O and –O–C═O bonds (Fig. S12). Moreover, the O 1 s for NaOOC-COF reveals C–O–C and –O–C═O (Fig. S14) comparison with NC-COF (Fig. S13). These results can further suggest the successful synthesis of NaOOC-COF. Thermal stability of prepared COFs is studied by thermogravimetric analysis (TGA). Both NC-COF and NaOOC-COF display superior thermal stability at 250 °C under $N_2$ atmosphere (Fig. S15). This excellent thermal stability of NaOOC-COF might play a crucial role in the long-term and safe using of battery.

The phase purity of synthesized NC-COF and NaOOC-COF is investigated by scanning electron microscopy (SEM). As a result, the NC-COF (Fig. S16) displays similar flake-like morphology [40,41]. In addition, transmission electron micrographs (TEM) images of NC-COF can further suggest the morphology (Fig. S17). After chemical modification for NC-COF material, the morphology of product NaOOC-COF is similar with the NC-COF proved by the SEM (Fig. 3a) and TEM (Fig. 3b). No metal particles can be found from the high resolution TEM image of NaOOC-COF (Fig. 3c), suggesting uniform Na-ions coated on the framework of NaOOC-COF. The elements content of NaOOC-COF are measured by energy-dispersive X-ray spectroscopy (EDS), revealing the content of 5.37 wt% Na in NaOOC-COF (Fig. S18), which is similar with the result of inductively coupled plasma evaluation (5.28 wt%). More importantly, EDS mappings imply that C, O and Na are uniformly dispersed in NaOOC-COF (Fig. 3d-g).

Fig. 4a shows the magnetic resonance $^{23}Na$ NMR spectrum of NaOOC-COF and a singlet presents at ~0.2 ppm, implying that Na-ions exist an equivalent chemical environment. Based on above results of successful preparation abundant Na-ions modified COF, we evaluate the electrochemical performance of NaOOC-COF. The Na-ion conductivity is carried out by the stainless-steel die. Self-standing pellet of NaOOC-COF is made by cold-pressing method. The synthetic pellet shows with proximate 200.0 μm thickness measured by a calliper. The interfacial contact always plays a crucial issue for the solid batteries between electrode and electrolyte, and the interfacial compatibility can be improved by some methods [35,43]. Consequently, for the outstanding interfacial contact of solid electrolyte and electrode, the liquid electrolyte (10.0 μL, 1.0 M) of $NaPF_6$ (in propylene carbonate, PC) was added into the NaOOC-COF solid electrolyte in order to enhance the interfacial contact and compatibility, promote the dissociation of COONa in COF and ultimate ion conduction [44,45].

Firstly, we measure the conductive behavior of Na-ions in NaOOC-COF using the electrochemical impedance spectroscopy (EIS), which is carried out at various temperatures from 20 °C to 80 °C. The Nyquist plot of NaOOC-COF does not demonstrate a semicircle at high frequency and a linear tail at low frequency at various temperatures (Fig. S19).

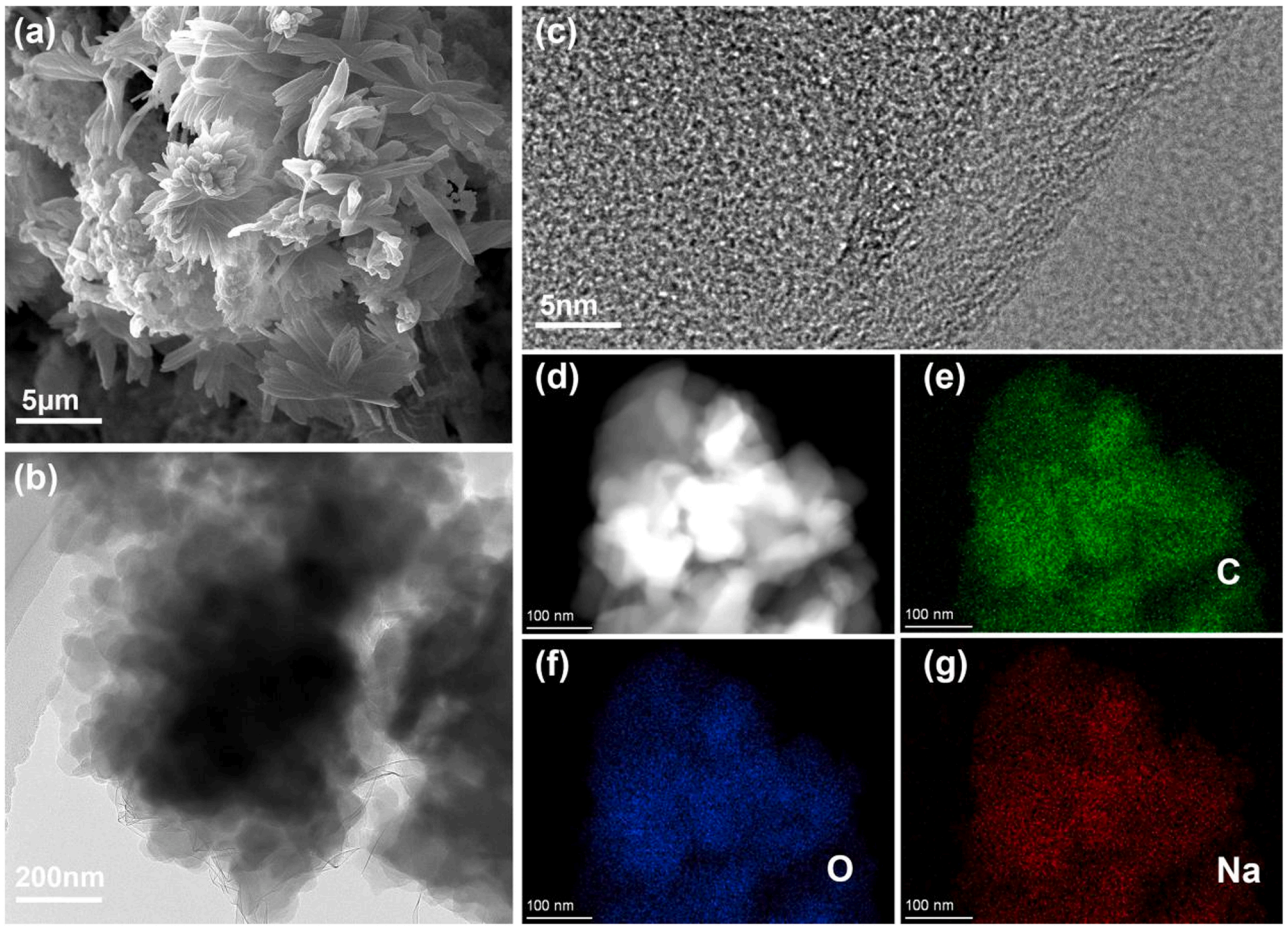


**Fig. 3.** SEM image of NaOOC-COF (a); TEM image of NaOOC-COF (b); high resolution TEM image of NaOOC-COF (c); EDS mappings of C, O and Na (d-g).

Because the semicircular impedance responses cannot be found in the EIS. Therefore, the respective resistance contribution of grain boundary and bulk is not divisional. Under the condition, the resistance is calculated by extrapolating the electrode spike to the "real" x-axis of the Nyquist plot (Fig. 4b) [35,46]. Consequently, ionic conductivity is creased with the enhance of temperature, affording values of $2.68 \times 10^{-4}$, $2.83 \times 10^{-4}$, $3.22 \times 10^{-4}$, $3.63 \times 10^{-4}$, $3.98 \times 10^{-4}$, $4.31 \times 10^{-4}$ S cm$^{-1}$ and $4.63 \times 10^{-4}$ S cm$^{-1}$ at 20, 30, 40, 50, 60, 70 and 80 °C for NaOOC-COF, respectively. As a result, a prominent advancement of NaOOC-COF is an ionic conductivity of $\sigma = 2.68 \times 10^{-4}$ S cm$^{-1}$ at 20 °C (Fig. S20). This excellent Na-ion ionic conductivity is the result of the well-defined ion channels of NaOOC-COF material and the favourably interfacial contact and compatibility supported by the negligible electrolyte addition. The Ea for NaOOC-COF can be obtained to be 0.24 V according to the Arrhenius plot (Fig. 4c), which suggests a proportional enhancement in the logarithmic ionic conductivity with an increase in heating [37 − 39]. The extraordinarily small Ea value is lower than previous works of Na-ions conductivity (Table S1), certifying the mobility pathway of Na-ions in NaOOC-COF with directional ion conduction pathways. The Na-ion conductivity of NaOOC-COF is compared to others polymer materials contained extra Na salts or solvent (Table S2), implying a superior ion conductivity performance at 20 °C. Notably, there are almost no researches based on Na-ion conductivity COF materials at present. Therefore, our results are mainly compared to others materials contained Na-ions conductivity and without COFs materials. This satisfied result generates from those facts that well-defined ion channels are constructed and abundant Na-ions are anchored in NaOOC-COF. In order to describe the Na-ion conduction behavior of NaOOC-COF, we assess its $t_{Na^+}$ using potentiostatic polarization strategy. A $t_{Na^+}$ value of 0.9 can be obtained from Fig. 4d, revealing the highlighted contribution of Na-ion to ion conductivity. Especially, the $t_{Na^+}$ value is obviously better than the reported Na-ions conductivity materials, benefiting from the structure advantage of NaOOC-COF with well-defined ion channels medication and abundant carboxylic acid sodium group embedding. Moreover, the excellent interfacial contact and compatibility between metal Na electrode and solid electrolyte NaOOC-COF are regulated by the $NaPF_6$. Although the presence of freely mobile anions $PF_6^-$, the NaOOC-COF is an anionic framework. Therefore, the anions $PF_6^-$ is repulsed by electrostatic interaction between $PF_6^-$ and NaOOC-COF. As a result, the quasi-solid-state NaOOC-COF conductor shows high $t_{Na^+}$ value. The detailed comparison with main focuses on these values of σ, Ea and $t_{Na^+}$ of our results with others Na-ions conductivity polymer electrolytes are shown in Table S2. Additionally, the electrochemical stability of Na-ion conductor is investigated using linear sweep voltammetry (LSV) test. As demonstrated in Fig. S21, an electrochemical stability window about 4.2 V is found for NaOOC-COF, suggesting correspondingly broad electrochemical window.

With the excellent ion conduction behavior in mind, we evaluate the practical application of NaOOC-COF that is acted as a fresh solid-state electrolyte for solid organic battery. The 1,4-benzoquinone (BQ) has attractively electrochemical performance as the cathode material in the batteries [47]. Nevertheless, the capacity dramatically decays and the cyclic performance is poor, which is caused by the dissolution of BQ in organic liquid electrolyte. These issues can be perfectly solved in the solid-state or quasi-solid-state batteries. We assemble the BQ | NaOOC-COF | Na quasi-solid organic Na-ion battery, which the BQ acts as the cathode, metal Na as the anode and the NaOOC-COF as solid

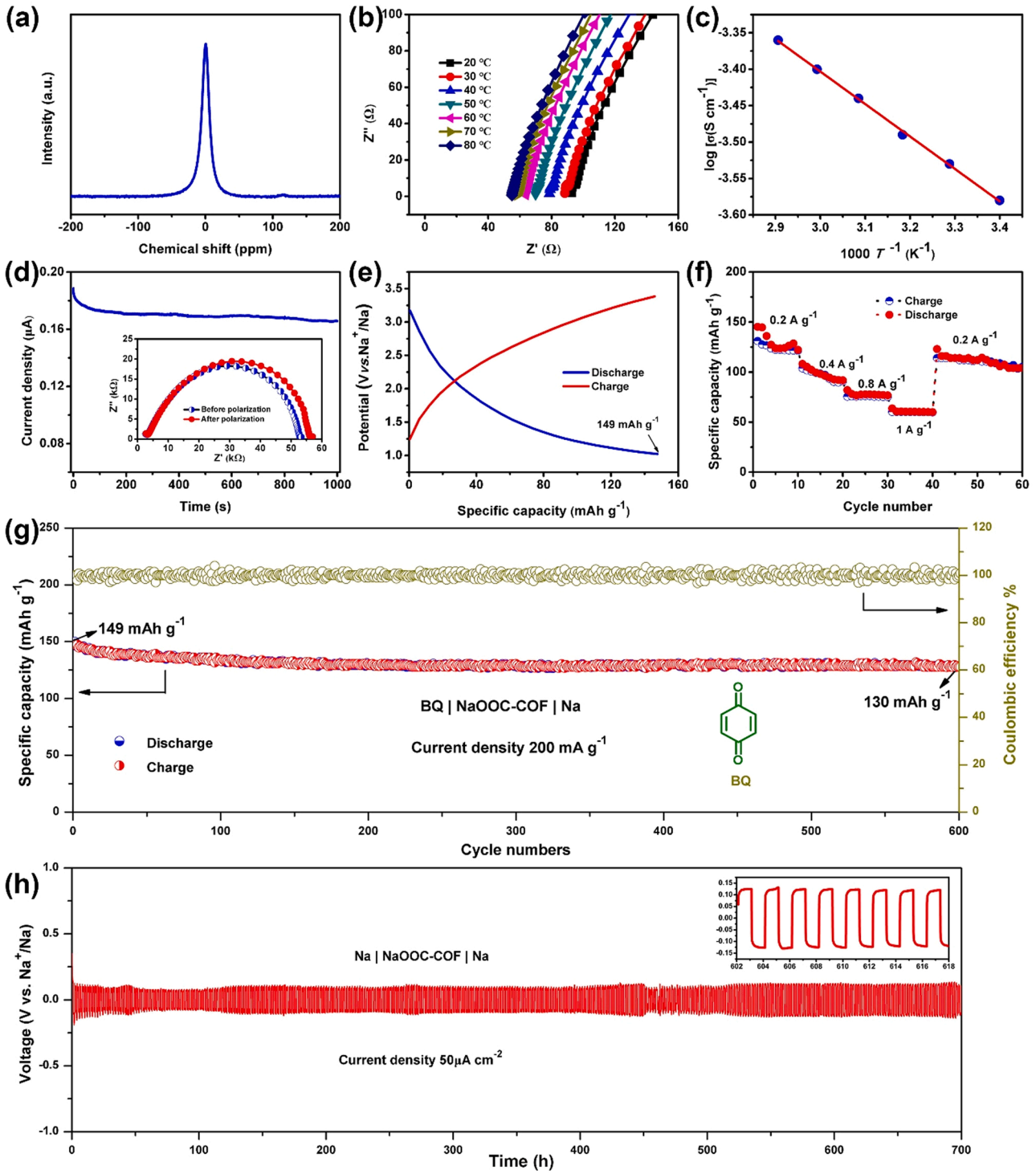


**Fig. 4.** Solid-state CP/MAS $^{23}$Na NMR characterization of NaOOC-COF material (a); EIS measurements made over a range of temperatures from 20° to 80°C (b); Arrhenius plot of ionic conductivity as a function of temperature (c); Na-ion transference number calculated using the Bruce-Vincent-Evans technique (d); galvanostatic charging-discharging curves of BQ | NaOOC-COF | Na cell at a current density of 200 mA $g^{-1}$ (e); charging-discharging profiles of BQ | NaOOC-COF | Na cell at different rates (f); cycling performance of BQ | NaOOC-COF | Na cell at current density of 200 mA $g^{-1}$ (g); Na stripping-plating test of Na | NaOOC-COF | Na at a current density of 50 μA $cm^{-2}$ for 1 h per cycle (h).

electrolyte. Similarly, the liquid electrolyte of $NaPF_6$ (10.0 μL, 1.0 M in PC) is added in order to enhance the interfacial contact and compatibility, promote the dissociation of COONa in COF and ultimate ion conduction. Fig. 4e displays the galvanostatic charging-discharging process at a current density of 200 mA $g^{-1}$, and the cathode material of BQ presents a discharging specific capacity of 149 mAh $g^{-1}$. In addition, the assembled battery has a salient rate performance at various current density (Fig. 4 f). More importantly, the BQ | NaOOC-COF | Na battery demonstrates outstanding cyclic performance for 600 cycles at current density of 200 mA $g^{-1}$ and 87.2% capacity retention (Fig. 4 g). However, by comparison, the assembled liquid organic electrolyte battery BQ | $NaPF_6$ | Na exhibits poor and unsatisfied cyclic and low capacity performance (Fig. S22) [48].

Moreover, we further study the NaOOC-COF performance in the Na/

Na symmetric battery configuration. Fig. 4 h illustrates the galvanostatic Na plating/stripping performance, which is tautologically conducted at a current density of 50 μA $cm^{-2}$ for 1 h each cycle. The constructed symmetric battery displays steady Na insertion/extraction processes for over 700 h without decrease and increase fluctuation of potential. Furthermore, the structure integrity of NaOOC-COF is not destroyed after the cycling measurement, indicating outstanding structural stability, confirmed by the FT-IR (Fig. S23) and PXRD tests (Fig. S24). This durability is the result of polyarylether linked hexahydroxytriphenylene framework, which shows superior chemical stability under various harsh chemical conditions (Fig. S25 and S26). In contrast, the symmetric battery without NaOOC-COF solid-state electrolyte displays unsteady Na insertion/extraction processes with obvious decrease and increase fluctuation of potential (Fig. S27).

We further study the surface of metal Na by the SEM technique. Both for the BQ | $NaPF_6$ | Na and Na | $NaPF_6$ | Na, the deposition of Na is ununiform by PP separator. Therefore, the dead Na or Na dendrite are observed by SEM technique on the surface of Na metal after cyclic tests in the liquid batteries (Fig. 5a, c and e) [49,50]. However, the COF with precise chemical modification and well-defined ion channels can impede the Na dendrite growth (Fig. 5b). The clean and smooth of Na metal electrode after cycles are confirmed by SEM (Fig. 5d and f), which Na deposition is hardly found, implying NaOOC-COF promotes homogeneous Na-ion migration toward the Na metal electrode. This compared test can further prove that NaOOC-COF has good solid-state electrolyte performance.

According to above excellent Na-ion conduction behavior, the mechanism of Na-ion migration is elucidated using density functional theory (DFT) calculations. In fact, the Na-ion migratory pathways are mainly orientations of perpendicular and parallel to cavizties of NaOOC-COF. The two orientations are marked as planar (Fig. 6a) and axial (Fig. 6b) approaches, respectively. Therefore, the different pathways of Na-ion migration are studied by investigation migration barriers at rate-determining steps under in axial and planar pathways (Fig. 6c and d) [33]. The optimized Na-ion geometries are applied to assess the initial state (IS) and final state (FS) (Fig. S28). In the both pathways, the O

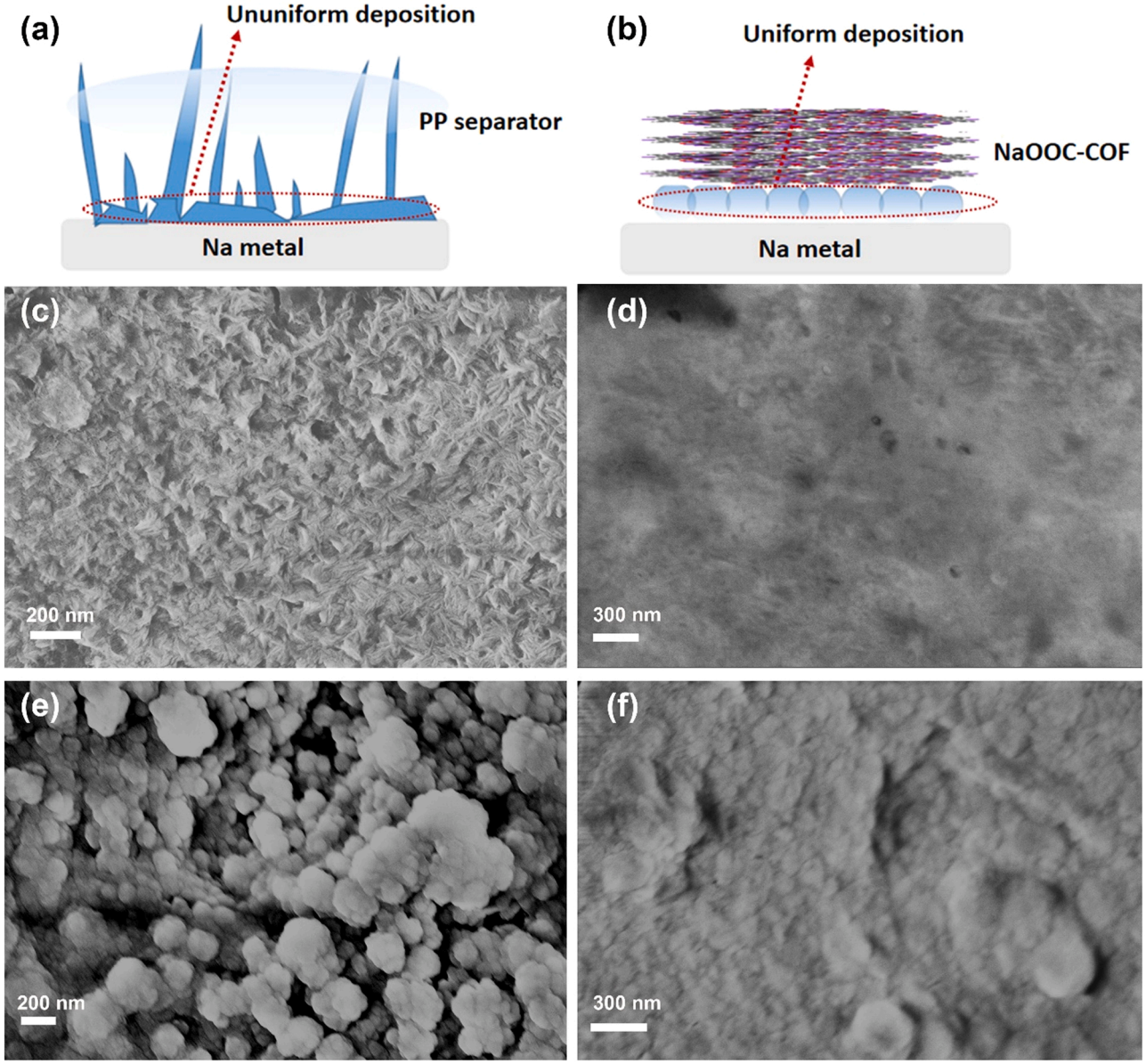


**Fig. 5.** Depiction of the Na ununiform deposition process on the PP separator (a) and uniform deposition on functionalized NaOOC-COF (b); SEM images of Na metal surface after test of BQ | $NaPF_6$ | Na and BQ | NaOOC-COF | Na at a current density of 200 mA $g^{-1}$ (c, d); SEM images of Na metal surface after test of Na | $NaPF_6$ | Na and Na | NaOOC-COF | Na at a current density of 50 μA $cm^{-2}$ (e, f).

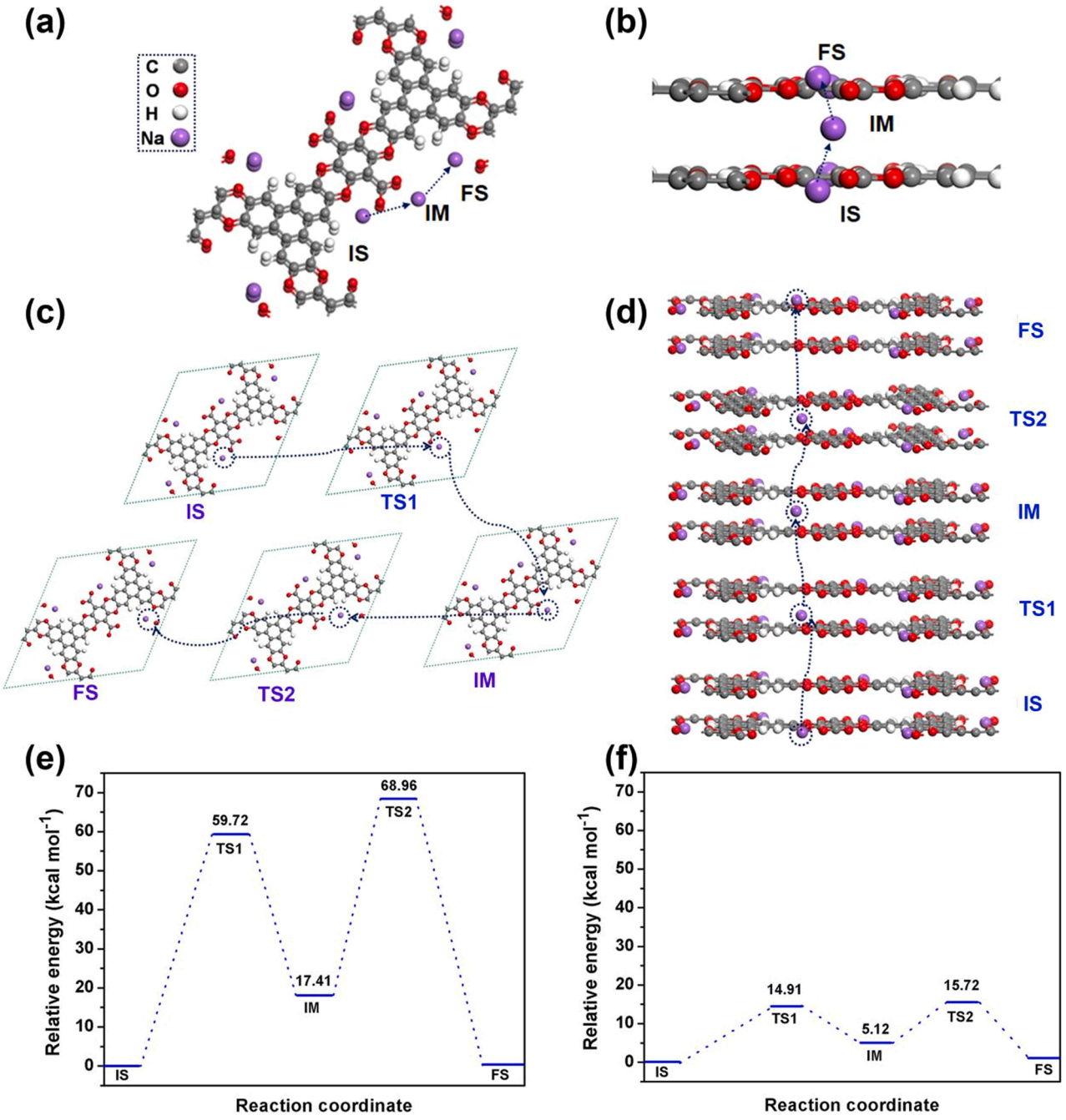


**Fig. 6.** Theoretical illustration of Na-ion migration behaviors inside the planar (a) and axial pathways (b); detailed theoretical elucidation of Na-ion migration behaviors inside the planar and axial pathways (c and d); migration barriers for planar (e) and axial pathways (f), respectively.

atoms of ether linkage in COF skeleton plays a crucial role for the movement of Na-ion via the cation-dipole interactions. As illustrated in Fig. 6e and f, after the hopping, a lesser migration barrier of 10.6 kcal mol$^{-1}$ (Fig. 6f) can be obtained along the axial pathway than the planar pathway of 51.5 kcal mol$^{-1}$ (Fig. 6e). This preferred axial migration pathway of Na-ion in the NaOOC-COF can be ascribed to the three facts: one is that the capacious pore of NaOOC-COF affords a more accessible environment than interplanar distance. This is because that cavity (1.6 nm) of NaOOC-COF is larger than Na-ion radius (0.23 nm). However, the interplanar distance (0.35 nm) is slightly larger than Na-ion (Fig. S29). Thus, the Na-ion migrates more easily in the pore. The other one is that the Na-ion migration during the axial pathway needs more short hopping distance than planar pathway, which is accelerated by the O atoms of ether linkage fragments (Fig. S29). This effect can promote the thermodynamic stability of Na-ion intermediates (IM1 and IM2) in the axial pathway, leading to beneficial aid for Na-ion migration. The last one fact is that the unique conjugated framework of p-π between O atom and hexahydroxytriphenylene centers, which leads to an integrated conjugated system of NaOOC-COF. This effect can weaken the electrostatic interaction of carboxylic acid sodium, and promote the dissociation between carboxylic acid anion and Na cation. Consequently, above theoretical analyses suggest that Na-ion directionally migrates along the stacked cavity of NaOOC-COF. Furthermore, the O atoms of ether linkage units offer a reliable assistance.

## 3. Conclusion

In summary, we have first explored the application of Na-ion

conductor supported by functionalized polyarylether conjugation covalent organic framework. The functional group of carboxylic acid sodium modified COF is reasonably designed and covalently tethered into the pores of COF to provide plentiful content of Na-ions and well-defined ion channels, which plays a reliable and solid foundation for Na-ion migration. The favourable structure promotes the direction Na-ion along the stacked pores of NaOOC-COF. Based on the framework uniqueness, allowing NaOOC-COF achieves exceptional Na-ion conductivity, particularly devoting to durable cycling performance of Na plating/stripping and excellent performance in solid organic battery. Our research contributes to a new solid-state electrolyte and Na metal battery for sustainable and inexpensive energy storage systems, which is in increasingly urgent demand of high-performance solid-state single-ion conductors. In the meantime, this study further broadens the applications and promotes the developments of covalent organic frameworks.

## Declaration of Competing Interest

The authors declare that they have no known competing financial interests or personal relationships that could have appeared to influence the work reported in this paper.

## Acknowledgments

The authors acknowledge financial support provided by the National Natural Science Foundation of China (52064049, 21467030 and 51764048), the Key National Natural Science Foundation of Yunnan Province (2018FA028 and 2019FY003023), International Joint Research Center for Advanced Energy Materials of Yunnan Province (202003AE140001), Key Laboratory of Solid State Ions for Green Energy of Yunnan University (2019), the Analysis and Measurements Center of Yunnan University for the sample testing service.

### *Supporting Information*

The chemical reagents, materials, characterized instruments, electrochemical tests, DFT calculation details, tables, and other supporting datas are described in the Supporting Information.

## Appendix A. Supporting information

Supplementary data associated with this article can be found in the online version at doi:10.1016/j.nanoen.2021.106756.

## References

[1] S. Chu, A. Majumdar, Opportunities and challenges for a sustainable energy future, Nature 488 (2012) 294–303.
[2] F. Hao, Y.L. Liang, Y. Zhang, Z.Y. Chen, J.B. Zhang, Q. Ai, H. Guo, Z. Fan, J. Lou, Y. Yao, High-energy all-solid-state organic–lithium batteries based on ceramic electrolytes, ACS Energy Lett. 6 (2021) 201–207.
[3] Y. Wang, W.D. Richards, S.P. Ong, L.J. Miara, J.C. Kim, Y. Mo, G. Ceder, Design principles for solid-state lithium superionic conductors, Nat. Mater. 14 (2015) 1026–1031.
[4] K. Xu, Electrolytes and interphases in Li-ion batteries and beyond, Chem. Rev. 114 (2014) 11503–11618.
[5] H.D. Yoo, Y.L. Liang, Y.F. Li, Y. Yao, High areal capacity hybrid magnesium–lithium-ion battery with 99.9% coulombic efficiency for large-scale energy storage, ACS Appl. Mater. Interfaces 7 (2015) 7001–7007.
[6] Y. Li, Y.-S. Hu, X. Qi, X. Rong, H. Li, X. Huang, L. Chen, Advanced sodium-ion batteries using superior low cost pyrolyzed anthracite anode: towards practical applications, Energy Storage Mater. 5 (2016) 191–197.
[7] N. Yabuuchi, K. Kubota, M. Dahbi, S. Komaba, Research development on sodium-ion batteries, Chem. Rev. 114 (2014) 11636–11682.
[8] H.S. Li, Y. Ding, H. Ha, Y. Shi, L.L. Peng, X.G. Zhang, C.J. Ellison, G.H. Yu, An all-stretchable-component sodium-ion full battery, Adv. Mater. 29 (2017) 1700898.
[9] H. Liu, H. Guo, B.H. Liu, M.F. Liang, Z.L. Lv, K.R. Adair, X.L. Sun, Few-layer $MoSe_2$ nanosheets with expanded (002) planes confined in hollow carbon nanospheres for ultrahigh-performance Na-ion batteries, Adv. Funct. Mater. 28 (2018) 1707480.
[10] H. Kwak, J. Lyoo, J. Park, Y. Han, R. Asakura, A. Remhof, C. Battaglia, H. Kim, S.-T. Hong, Y.S. Jung, $Na_2ZrCl_6$ enabling highly stable 3 V all-solid-state Na-ion batteries, Energy Storage Mater. 37 (2021) 47–54.
[11] H. Che, S. Chen, Y. Xie, H. Wang, K. Amine, X.-Z. Liao, Z.-F. Ma, Electrolyte design strategies and research progress for room-temperature sodium-ion batteries, Energy Environ. Sci. 10 (2017) 1075–1101.
[12] M.D. Slater, D. Kim, E. Lee, C.S. Johnson, Sodium-ion batteries, Adv. Funct. Mater. 23 (2013) 947–958.
[13] A.P. Cohn, N. Muralidharan, R. Carter, K. Share, C.L. Pint, Anode-free sodium battery through in situ plating of sodium metal, Nano Lett. 17 (2017) 1296–1303.
[14] Y. Zhao, V.L. Goncharova, A. Lushington, Q. Sun, H. Yadegari, B. Wang, W. Xiao, R. Li, X. Sun, Superior stable and long life sodium metal anodes achieved by atomic layer deposition, Adv. Mater. 29 (2017) 1606663.
[15] D. Lin, Y. Liu, Y. Cui, Reviving the lithium metal anode for high-energy batteries, Nat. Nanotechnol. 12 (2017) 194–206.
[16] C.L. Zhao, L.L. Liu, X.G. Qi, Y.X. Lu, F.X. Wu, J.M. Zhao, Y. Yu, Y.-S. Hu, L.Q. Chen, Solid-state sodium batteries, Adv. Energy Mater. 8 (2018) 1703012.
[17] J. Janek, W.G. Zeier, A solid future for battery development, Nat. Energy 1 (2016) 16141.
[18] X.-B. Cheng, R. Zhang, C.-Z. Zhao, Q. Zhang, Toward safe lithium metal anode in rechargeable batteries: A review, Chem. Rev. 117 (2017) 10403–10473.
[19] K. Fu, Y. Gong, G.T. Hitz, D.W. McOwen, Y. Li, S. Xu, Y. Wen, L. Zhang, C. Wang, G. Pastel, J. Dai, B. Liu, H. Xie, Y. Yao, E.D. Wachsman, L. Hu, Three-dimensional bilayer garnet solid electrolyte based high energy density lithium metal–sulfur batteries, Energy Environ. Sci. 10 (2017) 1568–1575.
[20] J.C. Bachman, S. Muy, A. Grimaud, H.-H. Chang, N. Pour, S.F. Lux, O. Paschos, F. Maglia, S. Lupart, P. Lamp, Inorganic solid-state electrolytes for lithium batteries: Mechanisms and properties governing ion conduction, Chem. Rev. 116 (2015) 140–162.
[21] Y. Zhu, X. He, Y. Mo, Origin of outstanding stability in the lithium solid electrolyte materials: Insights from thermodynamic analyses based on first-principles calculations, ACS Appl. Mater. Interfaces 7 (2015) 23685–23693.
[22] D.H.S. Tan, A. Banerjee, Z. Chen, Y.S. Meng, From nanoscale interface characterization to sustainable energy storage using all-solid-state batteries, Nat. Nanotech. 15 (2020) 170–180.
[23] A.P. Cote, A.I. Benin, N.W. Ockwig, M. Keeffe, A.J. Matzger, O.M. Yaghi, Porous, crystalline, covalent organic frameworks, Science 310 (2015) 1161–1170.
[24] X.G. Liu, D.L. Huang, C. Lai, G.M. Zeng, L. Qin, H. Wang, H. Yi, B.S. Li, S.Y. Liu, M. M. Zhang, R. Deng, Y.K. Fu, L. Li, W.J. Xue, S. Chen, Recent advances in covalent organic frameworks (COFs) as a smart sensing material, Chem. Soc. Rev. 48 (2019) 5266–5302.
[25] K. Geng, T. He, R. Liu, K.T. Tan, Z. Li, S. Tao, Y. Gong, Q. Jiang, D. Jiang, Covalent organic frameworks: Design, synthesis, and functions, Chem. Rev. 120 (2020) 8814–8933.
[26] K. Dey, S. Bhunia, H.S. Sasmal, C.M. Reddy, R. Banerjee, Self-assembly-driven nanomechanics in porous covalent organic framework thin films, J. Am. Chem. Soc. 143 (2021) 955–963.
[27] S.S. Yuan, X. Li, J.Y. Zhu, G. Zhang, P.V. Puyveldeb, B.V. Bruggen, Covalent organic frameworks for membrane separation, Chem. Soc. Rev. 48 (2019) 2665–2681.
[28] E. Vitaku, C.N. Gannett, K.L. Carpenter, L. Shen, H.D. Abruña, W.R. Dichtel, Phenazine-based covalent organic framework cathode materials with high energy and power densities, J. Am. Chem. Soc. 142 (2020) 16–20.
[29] G.F. Zhao, Y.H. Zhang, Z.H. Gao, H.L. Li, S.M. Liu, S. Cai, X.F. Yang, H. Guo, X. L. Sun, Dual active site of the azo and carbonyl-modified covalent organic framework for high-performance Li storage, ACS Energy Lett. 5 (2020) 1022–1031.
[30] S. Haldar, K. Roy, R. Kushwaha, S. Ogale, R. Vaidhyanathan, Chemical exfoliation as a controlled route to enhance the anodic performance of COF in LIB, Adv. Energy Mater. 9 (2019) 1902428.
[31] J. Liu, P.B. Lyu, Y. Zhang, P. Nachtigall, Y.X. Xu, New layered triazine framework/exfoliated 2D polymer with superior sodium-storage sroperties, Adv. Mater. 30 (2018) 1705401.
[32] G. Wang, N. Chandrasekhar, B.P. Biswal, D. Becker, S. Paasch, E. Brunner, M. Addicoat, M.H. Yu, R. Berger, X.L. Feng, A crystalline, 2D polyarylimide cathode for ultrastable and ultrafast Li storage, Adv. Mater. 31 (2019) 1901478.
[33] K. Jeong, S. Park, G.Y. Jung, S.H. Kim, Y.-H. Lee, S.K. Kwak, S.-Y. Lee, Solvent-free, single lithium-ion conducting covalent organic frameworks, J. Am. Chem. Soc. 141 (2019) 5880–5885.
[34] H.W. Chen, H.Y. Tu, C.J. Hu, Y. Liu, D.R. Dong, Y.F. Sun, Y.F. Dai, S.L. Wang, H. Qian, Z.Y. Lin, L.W. Chen, Cationic covalent organic framework nanosheets for fast Li-ion conduction, J. Am. Chem. Soc. 140 (2018) 896–899.
[35] Y.M. Hu, N. Dunlap, S. Wan, S.L. Lu, S.F. Huang, I. Sellinger, M. Ortiz, Y.H. Jin, S.-H. Lee, W. Zhang, Crystalline lithium imidazolate covalent organic frameworks with high Li-ion conductivity, J. Am. Chem. Soc. 141 (2019) 7518–7525.
[36] Q. Xu, S. Tao, Q. Jiang, D. Jiang, Designing covalent organic frameworks with a tailored ionic interface for ion transport across one-dimensional channels, Angew. Chem. Int. Ed. 59 (2020) 4557–4563.
[37] G. Zhang, Y.-L. Hong, Y. Nishiyama, S. Bai, S. Kitagawa, S. Horike, Accumulation of glassy poly(ethylene oxide) anchored in a covalent organic framework as a solid-state $Li^+$ electrolyte, J. Am. Chem. Soc. 141 (2019) 1227–1234.
[38] S. Chandra, T. Kundu, S. Kandambeth, R. BabaRao, Y. Marathe, S.M. Kunjir, R. Banerjee, Phosphoric acid loaded azo (–N=N–) based covalent organic framework for proton conduction, J. Am. Chem. Soc. 136 (2014) 6570–6573.
[39] Z. Xie, B. Wang, Z.F. Yang, X. Yang, X. Yu, G.L. Xing, Y.H. Zhang, L. Chen, Stable 2D heteroporous covalent organic frameworks for efficient ionic conduction, Angew. Chem. Int. Ed. 58 (2019) 15742–15746.

[40] X.Y. Guan, H. Li, Y.C. Ma, M. Xue, Q.R. Fang, Y.S. Yan, S. Valtchev, S.L. Qiu, Chemically stable polyarylether-based covalent organic frameworks, Nat. Chem. 11 (2019) 587–594.
[41] B. Zhang, M. Wei, H. Mao, X. Pei, S.A. Alshmimri, J.A. Reimer, O.M. Yaghi, Crystalline dioxin-linked covalent organic frameworks from irreversible reactions, J. Am. Chem. Soc. 140 (2018) 12715–12719.
[42] P.M. Hergenrother, The use, design, synthesis, and properties of high performance/high temperature polymers: an overview, High. Perform. Polym. 15 (2003) 3–45.
[43] X.Q. Zhu, K. Wang, Y.A. Xu, G.F. Zhang, S.Q. Li, C. Li, X. Zhang, X.Z. Sun, X.B. Ge, Y.W. Ma, Strategies to boost ionic conductivity and interface compatibility of inorganic-organic solid composite electrolytes, Energy Storage Mater. 36 (2021) 291–308.
[44] H. Gao, L. Xue, S. Xin, K. Park, J.B. Goodenough, A plastic–crystal electrolyte interphase for all-solid-state sodium batteries, Angew. Chem., Int. Ed. 56 (2017) 5541–5545.
[45] C.Q. Niu, W.J. Luo, C.M. Dai, C.B. Yu, Y.X. Xu, High-voltage-tolerant covalent organic framework electrolyte with holistically oriented channels for solid-state lithium metal batteries with nickel-rich cathodes, Angew. Chem. Int. Ed. 60 (2021) 2–10.
[46] Y. Zhang, J. Duan, D. Ma, P. Li, S. Li, H. Li, J. Zhou, X. Ma, X. Feng, B. Wang, Three-dimensional anionic cyclodextrin-based covalent organic frameworks, Angew. Chem. Int. Ed. 56 (2017) 16313–16317.
[47] Y. Wu, R. Zeng, J. Nan, D. Shu, Y. Qiu, S.-L. Chou, Quinone electrode materials for rechargeable lithium/sodium ion batteries, Adv. Energy Mater. 7 (2017) 1700278.
[48] X. Li, Q. Hou, W. Huang, H.-S. Xu, X.W. Wang, W. Yu, R.L. Li, K. Zhang, L. Wang, Z. G. Chen, K.Y. Xie, K.P. Loh, Solution-processable covalent organic framework electrolytes for all-solid-state Li−organic batteries, ACS Energy Lett. 5 (2020) 3498–3506.
[49] Q.W. Shi, Y.R. Zhong, M. Wu, H.Z. Wang, H.L. Wang, High-performance sodium metal anodes enabled by a bifunctional potassium salt, Angew. Chem. Int. Ed. 57 (2018) 9069–9072.
[50] L. Ye, M. Liao, T.C. Zhao, H. Sun, Y. Zhao, X.M. Sun, B.J. Wang, H.S. Peng, Inside cover: ultra-tuning of the aperture size in stiffened ZIF-8-Cm frameworks with mixed-linker strategy for enhanced $CO_2/CH_4$ separation, Angew. Chem. Int. Ed. 58 (2019) 2.

**Genfu Zhao** is currently a Ph.D. candidate of School of Materials and Energy in Yunnan University, China. He received his M.S. degree in Chemical Science and Technology, Yunnan University, China, in 2017. His research interests focus on COFs materials for advanced energy storage in LIBs and SIBs.

**Lufu Xu** is currently a graduate student of School of Materials and Energy in Yunnan University, China. He received his B.S. degree in School of Materials Science and Engineering, Nanchang Hangkong University, China, in 2019. His research interests focus on nano-materials for advanced energy storage in SIBs.

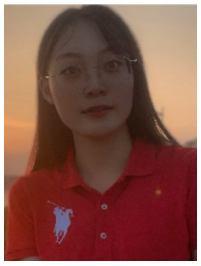

**Jingwen Jiang** is currently a graduate student of School of Materials and Energy in Yunnan University, China. She received his B.S. degree in School of Physics and Materials Engineering, Hefei Normal University, China, in 2020. Her research interests focus on nano-materials for advanced energy storage and conversion.

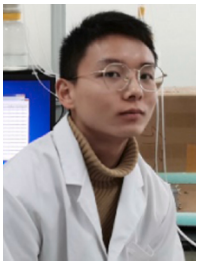

**Zhiyuan Mei** is currently a 2nd-grade postgraduate student at School of Materials and Energy, Yunnan University. He received his B. Eng. degree from Kunming University of Science and Technology in 2020. His research interests focus on design and synthesis in materials for Zinc-Air battery with high energy density and/or long term stability, especially for "M-$N_4$" structure materials.

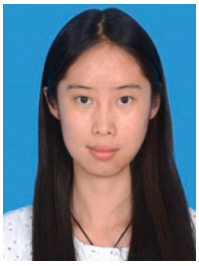

**Qi An** is currently a graduate student of School of Materials and Energy in Yunnan University, China. She received his B.S. degree in School of Materials Science and Engineering, Southwest Forestry University, China, in 2020. Her research interests focus on COFs materials for advanced energy storage in LIBs.

**Pengpeng Lv** is an Associate Professor at State Key Laboratory of Multiphase Complex Systems, Institute of Process Engineering, Chinese Academy of Sciences, China. He received his Ph.D. from University of Science & Technology Beijing in 2015. His research interests are focused on advanced materials for electrochemical energy storage and conversion, high-valued powders with surface modification.

**Dr. Xiaofei Yang** is currently a postdoctoral associate in Prof. Xueliang (Andy) Sun's Nanomaterials and Energy Group. He received his B.E. degree in Chemical Engineering from Anhui University, China, in 2013 and Ph.D. degree in Dalian Institute of Chemical Physics, Chinese Academy of Sciences, China, in 2018 under the supervision of Prof. Huamin Zhang. His research interests focus on all-solid-state Li-ion and Li-S batteries and battery interface studies via synchrotron X-ray characterizations.

**Hong Guo** is a Professor at Yunnan Key Laboratory of Micro/Nano Materials and Technology, School of Materials Science and Engineering, Yunnan University, China. He received his Ph.D. from University of Science & Technology Beijing in 2008. His research interests are focused on advanced materials for electrochemical energy storage and conversion, including electrode and solid-stateectrolyte materials for sodium-ion battery.

**Prof. Xueliang Sun** is a Canada Research Chair in Development of Nanomaterials for Clean Energy, Fellow of the Royal Society of Canada and Canadian Academy of Engineering and Full Professor at the University of Western Ontario, Canada. Dr. Sun received his Ph.D. in materials chemistry in 1999 from the University of Manchester, UK, which he followed up by working as a postdoctoral fellow at the University of British Columbia, Canada. His current research interests are focused on advanced materials for electrochemical energy storage and conversion, including electrocatalysis in fuel cells and electrodes in lithium-based batteries, metal-air batteries and solid-state batteries.